Talanta 99 (2012) 767–773

Contents lists available at SciVerse ScienceDirect

Talanta

journal homepage: www.elsevier.com/locate/talanta

SPR evaluation of binding kinetics and affinity study of modified RNA aptamers towards small molecules

Eva González-Fernández, Noemí de-los-Santos-Álvarez, Arturo José Miranda-Ordieres, María Jesús Lobo-Castañón *

Universidad de Oviedo, Departamento de Química Física y Analítica, Av. Julian Claveria 8, 33006 Oviedo, Spain

ARTICLE INFO

Article history:
Received 10 May 2012
Received in revised form
25 June 2012
Accepted 5 July 2012
Available online 16 July 2012

This work is dedicated to Professor Paulino Tuñón Blanco in honor of his retirement and in recognition of his career at Universidad de Oviedo.

Keywords:
Affinity constant
Endonuclease resistance
Kinetics
RNA aptamer
Surface plasmon resonance
Tobramycin

ABSTRACT

Establishing an efficient method for evaluating the affinity changes after post-SELEX modification of aptamers is essential for broadening the application of these oligonucleotides in biosensing. This is especially challenging when the ligand is a small molecule. Changes in affinity upon partial or total replacement of 2′–OH with 2′-OMe groups in the ribose moieties of a tobramycin binding RNA aptamer are described. The kinetic profile and binding properties of the different anti-tobramycin aptamers were measured by surface plasmon resonance (SPR) experiments through a real-time binding assay with the antibiotic covalently coupled to the gold sensor. This configuration maximizes the changes associated to the recognition event, which is otherwise undetectable. The results indicated that the modification slightly affects the binding characteristics of the parent RNA, while conferring biological stability to the aptamers against nucleases.

1. Introduction

The use of RNA or DNA aptamers as receptors for the development of biosensors and bioassays presents clear advantages derived from their superior thermal and chemical stability over antibodies and similar affinity. As synthetic single-stranded oligonucleotide sequences, their production is much simpler, faster, reproducible (chemical, no animal need) and it is not restricted to immunogenic or non-toxic targets. Since its discovery in 1990 [1,2], dozens of aptamers have been described mainly for therapeutic applications, and only a few have been used for sensing against targets to be analyzed in biological fluids. Although most aptamers known are RNA sequences, the vast majority of those used in analysis are DNA sequences because of their higher stability to hydrolytic digestion by nucleases.

Nucleases are enzymes able to catalyze the degradation of nucleic acids (DNA or RNA) by means of hydrolysis of phosphodiester bonds. They play a vital role in metabolism and are ubiquitous. In biological fluids, RNA sequences have life times of a few minutes [3] so, they are much more difficult to handle than DNA sequences. Fortunately, nucleic acids are very easy to modify in order to limit the degradation without affecting their affinity in sensing or activity in therapeutics. With this aim, several strategies focused on phosphate–sugar backbone modifications have been proposed.

Typical modifications of the phosphate backbone consist in replacing the non-binding oxygen in the phosphodiester linkage by sulfur (phosphorothioate) [4], phosphoramidate linkage and morpholino modifications [5,6]. Sugar modification is another widespread solution based on the replacement of the 2′-OH ribose position for *O*-Methyl, -F^-, -*O*-Methoxyethyl, -NH_2 groups using modified nucleotides during SELEX because their compatibility with polymerases. It has been demonstrated that changing 2′-OH group of ribose for 2′-NH_2 or 2′-F on pyrimidine nucleotides the nuclease resistance of the entire oligonucleotide is increased [7]. In 2005, the first fully 2′-*O* Me aptamer was raised by SELEX [8].

Additionally these sugar modifications can be introduced after SELEX at all or only selected nucleosides positions not directly involved in the molecular recognition event. This precludes performing a new SELEX for a given target. Toulmé et al. reported

Abbreviations: SELEX, Systematic Evolution of Ligands by EXponential Enrichment; VEGF, vascular endothelial growth factor; SPR, Surface Plasmon Resonance; MPA, 3-mercaptopropionic acid; EDC, N-(3-dimethylaminopropyl)-N′-ethyl-carbodiimide hydrochloride; NHS, N-hydroxysuccinimide; ATA, Anti-tobramycin aptamer; FATA, Fully 2′-*O*-methylated anti-tobramycin aptamer; NMATA, Non-*O*-methylated anti-tobramycin aptamer; SAM, self assembled monolayer; MTL, mass transport limitation; RII, refractive index increment

* Corresponding author. Tel.: +34 985106235; fax: +34 985103125.
E-mail address: mjlc@uniovi.es (M.J. Lobo-Castañón).

0039-9140/$ - see front matter © 2012 Elsevier B.V. All rights reserved.
http://dx.doi.org/10.1016/j.talanta.2012.07.019

a higher stability after fully 2′-*O*-methylation retaining the binding ability [9]. Nevertheless, rational selection of the modified positions can lead to significant improvement in affinity. It has been reported that fully modification of purines of an anti-VEGF aptamer led to a reduction in affinity whereas the selective modification of 10 out of 14 purines led to a 17-fold increase [10]. So, in order to use a modified aptamer for sensing it is of crucial importance reevaluating the affinity to verify the ability of these modified aptamers to recognize their target molecule.

Our group pioneered the use of 2′-*O*Me RNA aptamers for sensing in biological fluids. It was shown that a native RNA raised against neomycin B can be fully *O* methylated retaining enough affinity and selectivity to be used as receptor for the detection of the antibiotic in milk by impedance [11] or surface plasmon spectroscopy [12]. Recently, the aminoglycoside tobramycin was successfully detected in serum using a fully *O*-methylated aptamer [13], although the 2′–OH position of U12 was previously described to be involved in the molecular recognition event [14]. Preliminary estimations of the affinity constant by faradaic impedance spectroscopy resulted in similar values for both the fully *O*-methylated and the fully-but-one (U12) *O*-methylated aptamer. No comparison with the native one was carried out [13]. Although the fully 2′-*O*Me aptamer performance was satisfactory, an in-depth study about the affinity and binding kinetics between tobramycin and aptamer derivatives is lacking.

Herein, the affinity of the previously described natural RNA anti-tobramycin aptamer [15] was compared with aptamers with different 2′-*O*Me level at 2′-OH positions in order to understand its influence on affinity towards its target molecule, tobramycin. Surface plasmon resonance (SPR), a technique well suited for the characterization of affinity events that allows real-time monitoring of binding kinetics was used. The rate and equilibrium constants for the natural and the modified anti-tobramycin aptamers are given.

2. Materials and methods

2.1. Instrumentation

A double-channel cuvette-based SPR instrument equipped with an autosampler (Autolab-ESPRIT, Ecochemie, The Netherlands) was used for all SPR experiments. The instrument was controlled by Data Adquisition Software (ESPRIT version 4.4). Data treatment (overlapping and alignment of sensorgrams, zeroing and baseline corrections) and non-linear fitting of the resulting sensorgrams were done with the software provided with the instrument (ESPRIT kinetic evaluation version 5.2). Other non-linear fitting needed for data processing were carried out using OriginPro 7.5 (Northampton, MA). All SPR experiments were carried out using commercial BK7 disks coated with a 50 nm gold film supplied by Autolab (Metrohm, The Netherlands) under controlled temperature conditions of $25 \pm 1^{\circ}$ C obtained with a thermostat, Haake D1 (Germany).

2.2. Reagents

Three different types of 27-mer anti-tobramycin RNA aptamer were used throughout this work, which differ in the number of bases modified with *O*-methyl group at 2′-OH position of their ribose. All of them were synthesized by Sigma-Genosys (France) and purified by HPLC. Their sequences are the following:

Anti-tobramycin aptamer (ATA): 5′ [mG] [mG] [mC] [mA] [mC] [mG] [mA] [mG] [mG] [mU] [mU] U [mA] [mG] [mC] [mU] [mA] [mC] [mA] [mC] [mU] [mC] [mG] [mU] [mG] [mC] [mC] 3′

Fully 2′-*O*-methylated anti-tobramycin aptamer (FATA): 5′ [mG] [mG] [mC] [mA] [mC] [mG] [mA] [mG] [mG] [mU] [mU] [mU] [mA] [mG] [mC] [mU] [mA] [mC] [mA] [mC] [mU] [mC] [mG] [mU] [mG] [mC] [mC] 3′

Non-*O*-methylated anti-tobramycinaptamer (NMATA): 5′G G C A C G A G G U U U A G C U A C A C U C G U G C C 3′

Tobramycin sulfate, 3-mercaptopropionic acid (MPA), N-(3-dimethylaminopropyl)-N′-ethyl-carbodiimide hydrochloride (EDC), N-hydroxysuccinimide (NHS) were purchased from Sigma-Aldrich (Spain). 4-(2-hydroxyethyl)-piperazine-1-ethanesulfonic acid (HEPES), ethanolamine, salts for buffer solutions (KCl, NaCl, $MgCl_2$, $CaCl_2$), 1 M Tris/HCl pH 7.4 solution and HCl (all RNAse free) were also obtained from Sigma-Aldrich (Spain). All other reagents were of analytical grade.

All glassware in direct contact with aptamer was previously cleaned with RNAseZAP^{TM} (Sigma-Aldrich, Spain) and all aqueous solutions were prepared with RNAse free water purified by a Direct-Q system with a BioPack cartridge (Millipore).

The compositions of the buffers used for the experiments are as follows:

Immobilization solution: 0.1 M HEPES pH 8.64.

Affinity solution: 20 mM Tris–HCl pH 7.4, 140 mM NaCl, 5 mM KCl, 1 mM $MgCl_2$, 1 mM $CaCl_2$.

Regeneration solution: 0.05 M HCl.

2.3. Tobramycin immobilization protocol

Initially the bare gold-coated glass sensor was cleaned by immersion in piranha solution (3 H_2SO_4 (95%):1 H_2O_2 (33%)) (CAUTION: piranha solution is strongly oxidizing and should be handled with care!) for 10 min, thoroughly rinsed with water and ethanol, and dried with a stream of N_2. Then the sensor was positioned onto the clean hemi-cylinder lens previously coated with a drop of immersion oil (Autolab, Methrom, The Netherlands), which possesses a constant refractive index ($n_D^{25^{\circ}C} = 1.518 \pm 0.002$). Afterwards, water was injected in both channels and the surface was equilibrated until a constant response was obtained.

The sensing phase preparation entails the covalent immobilization of tobramycin onto a self-assembled monolayer of MPA on gold, following a protocol similar to that previously described [12]. Briefly, the SAM was formed overnight after manually injection of 40 mM MPA prepared in an ethanol:water solution (75:25). After washing with ethanol and water, the sensor surface was equilibrated with water and the covalent attachment of tobramycin (channel 1) and ethanolamine (channel 2, reference) was carried out. The ESPRIT autosampler and sequencer allowed the simultaneous modification of both channels. The procedure consisted in a three-step sequence: (1) Surface activation: three consecutive injections of a mixture of 0.2 M EDC and 0.05 M NHS in water for 5 min each one, followed by a brief washing step with water. (2) Binding step: three consecutive injections of 10 mM tobramycin (channel 1) and 1 M ethanolamine (channel 2) prepared in immobilization solution for 20 min each one, followed by a brief washing step with water. (3) Blocking step: one injection of 1 M ethanolamine prepared in immobilization solution in both channels for 30 min.

Finally the modified surface was equilibrated with affinity solution.

2.4. SPR measurements

All binding experiments were carried out in affinity buffer, the same used in the anti-tobramycin SELEX selection [15]. Due to the cuvette-based design of the ESPRIT instrument, constant stirring conditions are required for controlling hydrodynamic properties of the system. The whole data collection process is automated and consisted in recording successive cycles of measurement. Each independent analysis cycle includes baseline, association, dissociation, regeneration and back to baseline steps as follows. After obtaining a stable signal by acquiring several baselines, varying

concentrations of aptamer prepared in affinity buffer (35 μL) were simultaneously injected in both channels by means of the ESPRIT autosampler and the association phase was recorded for 10 min. After draining the cuvette, 50 μL of affinity buffer was injected and the dissociation phase was monitored for 5 min resulting in the decrease of the signal until a stable value was achieved. Finally regeneration step was accomplished by several injections of 50 μL of 0.05 M HCl (1 min) followed by baseline registration until the initial value was reached.

2.5. Fitting models

For both kinetics and equilibrium analysis, non-linear fitting of the association phase was used for interpreting data. In the basis of a bimolecular interaction model (1:1 stoichiometry), the R_t is described by the integrated Eq. (1).

$$R_t = \frac{R_{\max}[aptamer]k_{on}}{k_{on}[aptamer]+k_{off}}(1-\exp^{-(k_{on}[aptamer]+k_{off})t})+R_0 \quad (1)$$

where, R_{max} is the maximum angle shift in m°, a measure of the maximum binding capacity when all binding sites on the sensor surface are occupied; R_0 is the angle shift at $t=0$; [*aptamer*] is the concentration of the analyte; k_{on} and k_{off} are the association and dissociation rate constants of the complex tobramycin–aptamer, respectively. This equation can be simplified to Eq. (2):

$$R_t = R_0+E(1-\exp^{-k_s t}) \quad (2)$$

where, $R_0+E=R_{eq}$ for each aptamer concentration and $k_s=k_{on}[aptamer]+k_{off}$

2.5.1. Equilibrium model

R_{eq} values were estimated from the non-linear fitting to Eq. (2). Plotting R_{eq} against free aptamer concentration, a Langmuir binding isotherm is obtained (Eq. (3)).

$$R_{eq} = R_{max}\left(\frac{[aptamer]_{free}}{[aptamer]_{free}+K_D}\right) \quad (3)$$

A frequent way of estimating K_D is linearizing Eq. (3), which leads to a Scatchard plot, described by Eq. (4).

$$\frac{R_{eq}}{[aptamer]_{free}} = K_A R_{\max} - K_A R_{eq} \quad (4)$$

where K_A is the equilibrium association constant. This way, K_D is estimated as the reverse value of the slope (K_A) of Eq. (4).

2.5.2. Kinetic model

Fitting the association phase for all sensorgrams to Eq. (2) provide an apparent rate constant, k_s value for each aptamer concentration. The plot of k_s versus $[aptamer]_{free}$ should give a linear function. k_{on} is obtained from the slope of the plot and k_{off} from the intercept. Although k_{on} is accurately estimated, in practice, large errors are associated to k_{off} estimation for this method [21]. A more precise method is to obtain k_{off} from non-linear fitting of the dissociation phase of the sensorgrams, which is a first-order exponential decay with an offset, R_∞ that indicates the angle shift after decay is finished (Eq. (5)), that accounts for the incomplete dissociation characteristic of cuvette-based SPR instruments.

$$R_t = R_0 e^{-kdt} + R_\infty \quad (5)$$

3. Results and discussion

Different aptamers have been described in literature to specifically recognize the antibiotic tobramycin [15–18]. The most recent one was a DNA aptamer raised against kanamycin, a closely structurally related antibiotic, which showed cross-reactivity with tobramycin as similar K_D values about 100 nM for both of them unambiguously indicate [18]. The rest of them are RNA aptamers. A beacon aptamer evolved against tobramycin showed a very high K_D of 16 μM, although the need for further optimization of the SELEX process is recognized [16]. Using automated SELEX three aptamers were found for tobramycin with K_D ranged between 10 and 100 nM [17]. Finally, Wang and Rando [15] have found two different consensus sequences with affinity for tobramycin, and some degree of homology with K_D of 12 nM and 9 nM. The last one was chosen to carry out this work based on its high affinity. As mentioned above, in order to preclude the enzymatic hydrolysis caused by nucleases towards RNA an internal modification on sugars was performed. Thus, the hydroxyl group at the 2′-position of the ribose ring in the bases was replaced by an *O*-methyl group. In this context two different modified aptamers were designed. The first one included the sugar modification in all its 27 bases, and it was referred as fully modified anti-tobramycin aptamer (FATA). The 2′-OH of the U base at 12 position was reported to be involved in the formation of a hydrogen bond with N7 of G14, which has a relevant contribution in the definition of the hairpin 3D conformation for proper tobramycin recognition. So, a second modified anti-tobramycin aptamer was designed where the U-12 conserved its native unmodified ribose. This aptamer was referred as anti-tobramycin aptamer (ATA). The native, non-*O*-methylated anti-tobramycin aptamer (NMATA) was also used for comparison in terms of its equilibrium (K_D) and rate constants (k_{on}, k_{off}).

A typical SPR assay involves the immobilization of one of the interacting partners onto the sensor surface, which is exposed to a solution containing the other component. To decide which compound will be immobilized on the surface, size, stability, solubility and functional groups available should be taken into consideration. In our particular case, the critical parameter was the size because the SPR response is highly dependent on the mass of the interacting molecule. Molecules smaller than 1000 Da do not provide a significant change in the refractive index on a surface with limited binding sites, so, they are difficult to detect with sufficient accuracy. Although in some cases this lack of sensitivity can be overcome by increasing the molecule density on the surface, very high densities are not convenient for kinetic studies as explained below.

Consequently, immobilization of the smaller partner (tobramycin, the ligand) was preferable to maximize the SPR response (Fig. 1). However, this configuration can be a source of mass transport limitation (MTL) because the aptamer, a molecule of relatively high mass, is added to the cuvette and has to diffuse towards the sensor surface. MTL appears when the binding rate is faster than the diffusion rate from the bulk to the surface and affects to the same extent both association and dissociation phases. The higher binding sites concentration the higher consumption of aptamer at the surface, making more evident the MTL contribution. This effect is minimized by constructing low capacity binding surfaces. When working with interactions with k_{on} (association rate constant) $\geq 10^6\ M^{-1}\ s^{-1}$ [19], MTL has to be incorporated into the model of the binding kinetics for an adequate evaluation. Nevertheless, a self-consistency test is always a healthy behavior when interpreting kinetic data.

In this study, low amounts of bound tobramycin led to adequate sensing surfaces for kinetic analysis considering first-order kinetics. The angle shifts obtained for different sensing surfaces after tobramycin immobilization (R_{tob}) were in the range of 15–30 m°, which corresponds to 141–282 pg mm^{-2} of antibiotic. This value was calculated taking into account that 120 m° corresponds to 1 ng mm^{-2} of bound protein or 1.13 ng mm^{-2} of

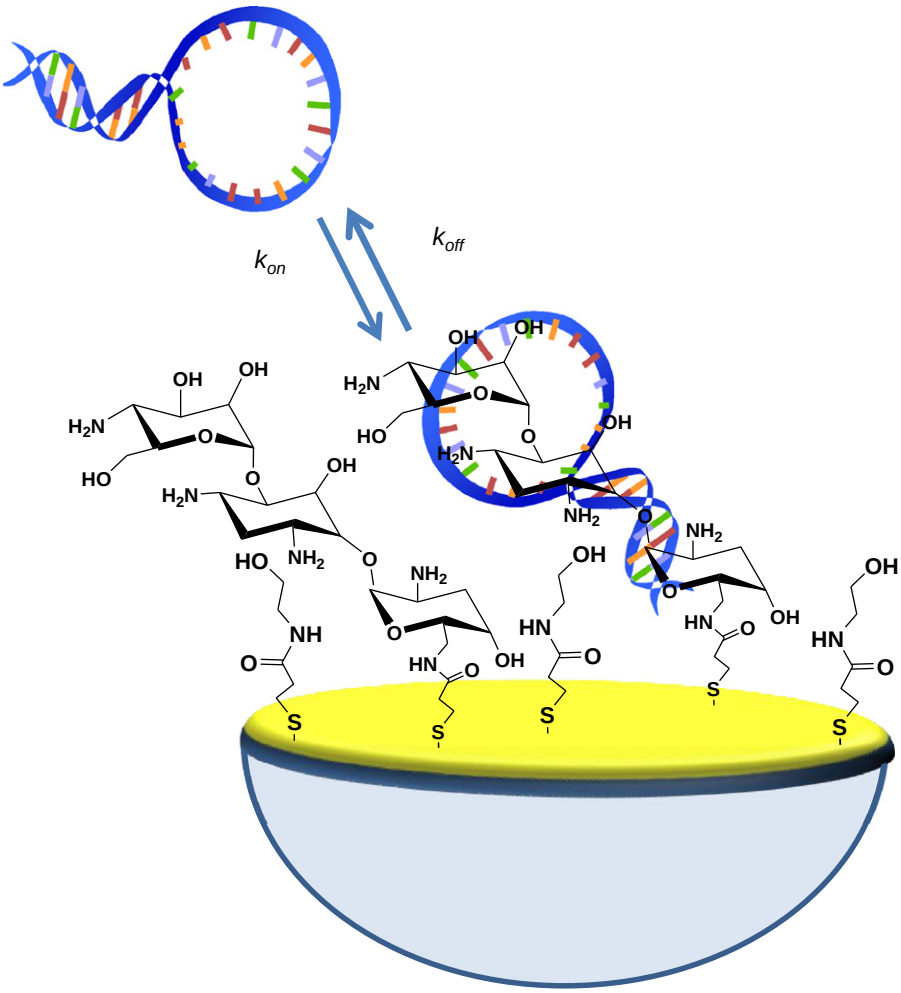

Fig. 1. Scheme of the sensing phase employed for SPR binding assays.

bound tobramycin considering the refractive index increment (RII) between proteins and aminoglycoside antibiotics [20].

The interaction of immobilized tobramycin with different concentrations of aptamer in solution was monitored, and subsequently processed and analyzed for obtaining both kinetics and equilibrium information. Binding curves were performed for each aptamer ATA, FATA and NMATA, recording an analysis cycle for each concentration assayed, in the range of 0.05–3 μM, ensuring the equilibrium is reached in all the experiments.

When injecting the aptamer solution the amount of the aptamer–tobramycin complex formed was monitored as variation of the resonance angle (angle shift, R_t) with time (sensorgram) as that depicted in Fig. 2 for each aptamer. After each injection a rapid signal increase was observed due to bulk effects related to the change in composition of the solutions injected. It is worth noting that only in channel 1, a progressive increase in the angle shift is observed whereas a constant and almost negligible angle shift is recorded in channel 2. This is a clear indication that aptamer effectively binds to tobramycin on the surface of channel 1 that contains the antibiotic, and the amount of unspecific binding to ethanolamine-blocked mercaptopropionic acid SAM (channel 2) is negligible because there are not tobramycin. After flushing out the aptamer solution and filling the cuvette with affinity solution, the angle shift did not return to the baseline level in channel 1 indicating that the aptamer is specifically bound to the sensor surface. The decrease is related to the dissociation of the complex that occurs in a certain extent. In contrast, in channel 2, the angle shift remains at the baseline level confirming that there is no aptamer unspecifically bound in the absence of immobilized tobramycin. Finally, regeneration of the surface under mild acidic conditions removed the entire surface complex without affecting the SAM stability significantly, and a new cycle can be performed.

When the concentration of aptamer increased (Fig. 3), both the slope of the angle shift (R_t) and the signal at equilibrium (R_{eq}) were higher indicating that higher amounts of aptamer are retained by the modified surface. The sensing phase can be regenerated several times and an entire binding experiment can be carried out with the same surface (see Fig. S1 in Supporting Information).

This set of SPR data contains both kinetics and equilibrium information about the biomolecular interaction under study. The kinetic rate constants (k_{on} and k_{off}) and equilibrium constants provide valuable information about the affinity of the interaction. The equilibrium constant can be estimated from both kinetic and equilibrium data being necessary a convergence value as a self-consistency test.

The association phases of sensorgrams obtained for each aptamer at different concentrations were fitted to Eq. (2) (Fig. 3, white lines). In cuvette-based instruments as used in this work, a depletion of the aptamer concentration can occur due to the loss of material derived from the binding event in contrast to flow systems where a continuous supply of compound exists. This effect was quantified and corrected by calculating the free analyte concentration employing Eq (6) [21].

$$[aptamer]_{free} = [aptamer]_0 - \frac{R_{eq}\, S\, 10^{-3}}{f\ MW\, V} \tag{6}$$

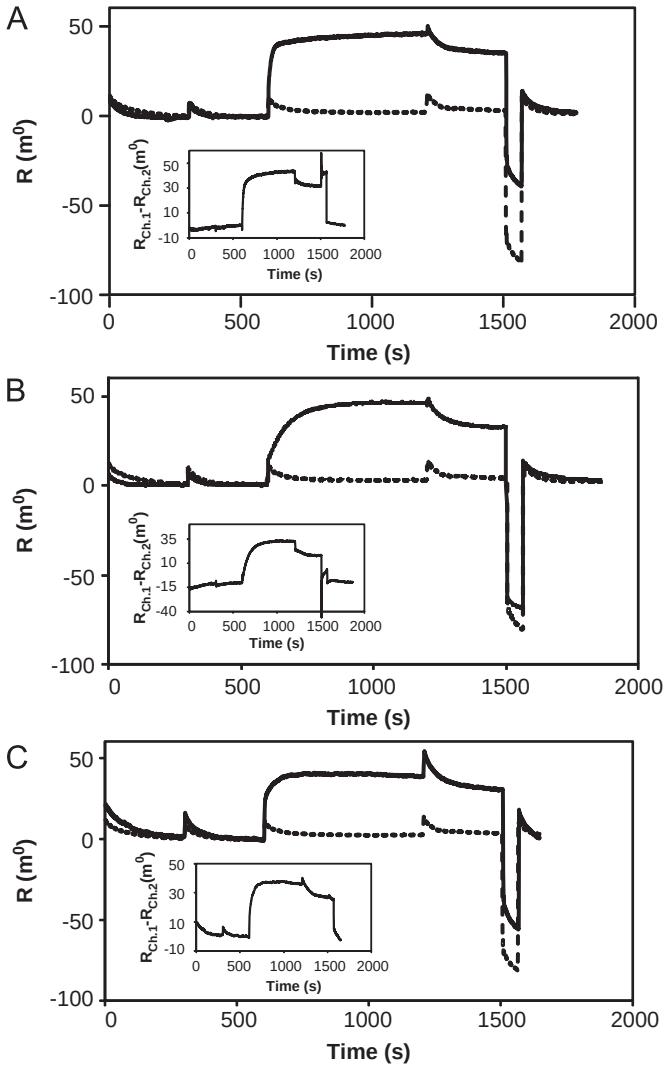

Fig. 2. Sensorgrams showing a full analysis cycle including two baselines, association, dissociation, regeneration and back to baseline steps for a tobramycin-modified surface (channel 1, solid line) and for an ethanolamine-modified surface (channel 2, reference, dashed line) using (A) 0.5 μM NMATA, (B) 0.3 μM ATA and (C) 0.75 μM FATA. See text for details about the buffers used. Inset: Substracted sensorgram (channel 1 minus channel 2) for each cycle.

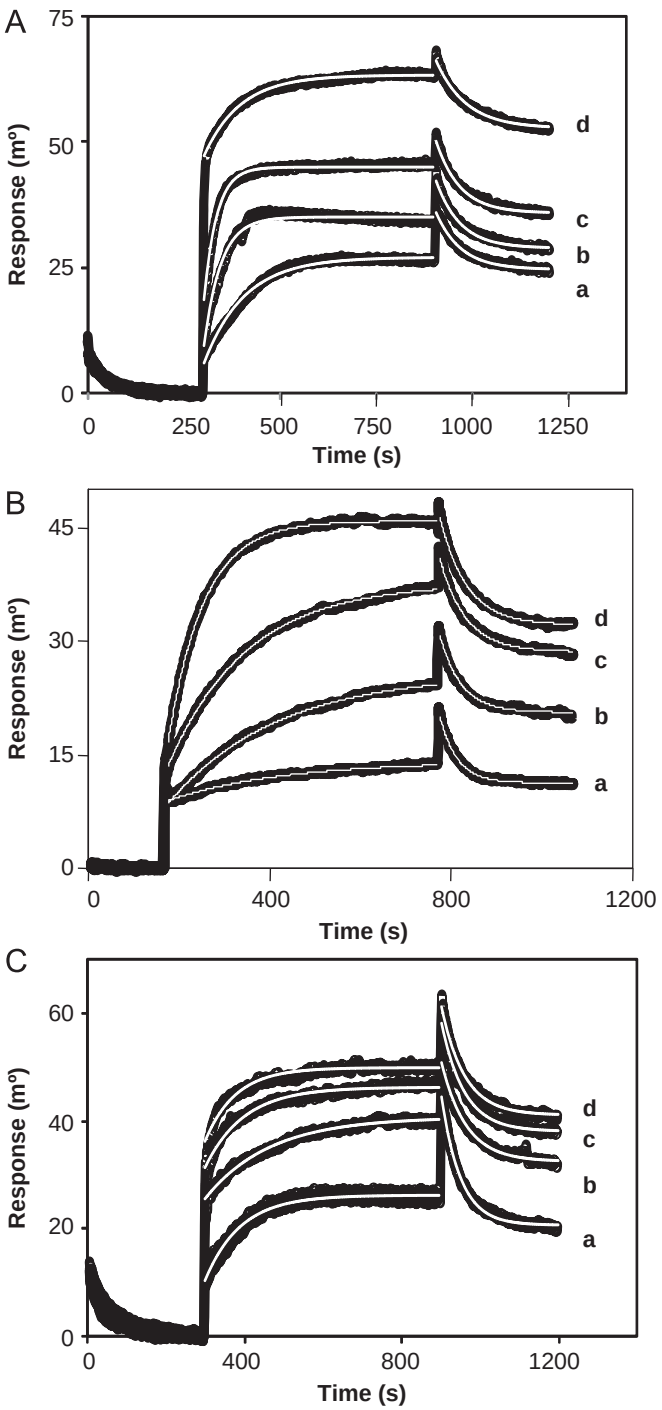

Fig. 3. Overlays of SPR sensorgrams registered for the addition of (A) NMATA at (a) 0.05; (b) 0.1; (c) 0.25 and (d) 1 μM; (B) ATA at (a) 0.08; (b) 0.1; (c) 0.15 and (d) 0.3 μM; (C) FATA at (a) 0.2; (b) 0.5; (c) 1 and (d) 1.5 μM (black lines) in affinity buffer (see text for details). Non-linear curve fitting to association and dissociation phases (white lines).

where, $[aptamer]_0$ is the added aptamer concentration in molar; $[aptamer]_{free}$ is the corrected aptamer concentration also in molar; S is the surface of the sensor in contact with bulk solution (2.8 mm^2); f=120 m°/0.8 ng mm^{-2} is the conversion factor between the measured angle shift in m° and the mass density of bound aptamer in ng mm^{-2}, MW is the molecular weight of the aptamer and V is the sample volume injected (35 μL in all cases). This correction was taken into account in all subsequent calculations.

For depletion values larger than 10% of the initial analyte concentration, the amount of free analyte decreases considerably during association phase and second-order equations better describe the binding event [22]. Depletion values were below 5% of the initial aptamer concentration in all experiments being more important for the lower concentrations tested. So, first-order equations were used for calculations.

3.1. Equilibrium analysis

Langmuir binding isotherms were obtained for each aptamer using the R_{eq} values estimated from the non-linear fitting to Eq. (2) (Fig. 4). Values of K_D were calculated from the corresponding Scatchard plots (inset Fig. 4) and displayed in Table 1.

It is well-known that Scatchard plot can lead to important errors in K_D evaluation [21] thus, in this study K_D values were also estimated directly by non-linear fitting of Eq. (3) and compared (Langmuir isotherm).

From them, it is clear that all K_D values corresponding to different *O*-methylated aptamers (ATA, FATA and NMATA) are in the subμM range. Likewise, both Scatchard plot and non-linear

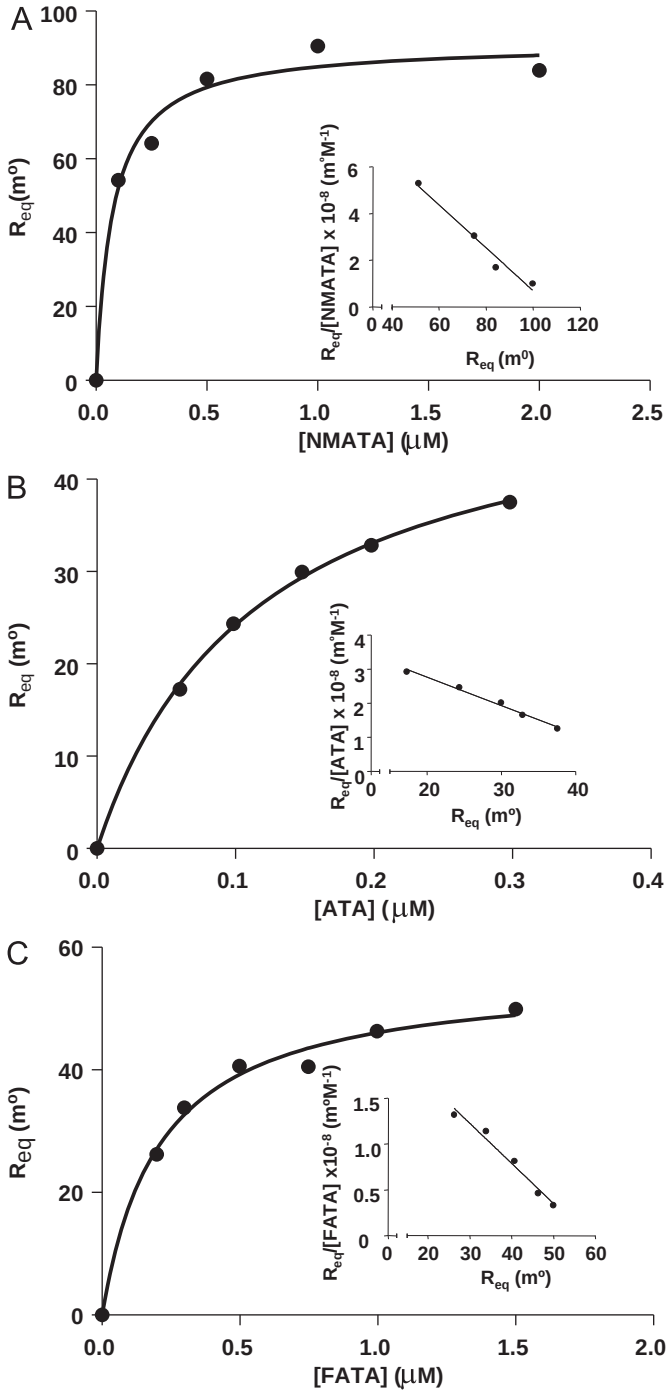

Fig. 4. Binding isotherms obtained with a tobramycin modified sensor after incubation with increasing concentrations of (A) NMATA (B) ATA and (C) FATA in affinity buffer for 10 min. Inset: Scatchard plot for each set of experiments.

fitting to Langmuir binding isotherm have led to similar K_D values for each individual aptamer. The lowest K_D value (below 100 nM) corresponded to the original, non-*O*-methylated anti-tobramycin aptamer, NMATA. The modified aptamers tested showed K_D values above 100 nM. ATA exhibits a slightly lower K_D (stronger binding) compared with FATA. From these results it can be stated that the affinity tends to diminish when the level of *O*-methylation increases. However, this trend is not very large, about 4-fold decrease for total substitution. As mentioned above, NMR measurements and computed structures of the tobramycin–NMATA complex suggest the stabilizing role of a hydrogen bond between 2′-OH of U12 and N7 of G14. Although useful, this information does not provide quantitative information about the magnitude of the destabilization when this hydrogen bond is blocked. In this study, this effect was quantified in terms of K_D values, to be about 1.5-fold decrease in addition to the reduction observed after modifying the other 26 nucleosides (ATA). This is a modest effect in affinity that can be overcome by the gain in nuclease resistance, which is in good agreement with the feasibility of using FATA for tobramycin detection in human serum [13].

3.2. Kinetic analysis

SPR data were also used to determine the kinetic parameters for tobramycin binding to all three aptamers under study. The dissociation constant was evaluated from these kinetic parameters and compared with the previously obtained by means of equilibrium data.

Table 2 compiles all rate constants obtained for each aptamer. For all three aptamers tested k_{on} values are below $10^6\ M^{-1}\ s^{-1}$, which confirmed the applicability of the initial assumption of a simple bimolecular model with no MTL [19]. Both k_{on} and k_{off} change slightly with the degree of *O*-methylation, favoring NMATA over ATA and FATA (k_{on} larger and k_{off} smaller in a similar amount). According to expression $K_D = k_{off}/k_{on}$, the dissociation constant was estimated.

It has been argued that k_{off} values obtained under conditions that the dissociation is not complete (such as in this case) could deviate from the real value. Such an incomplete dissociation can be due to two causes: MTL, which was discarded from the k_{on} value or rebinding, which is always present in cuvette-based instruments even under conditions that MTL does not apply. Another alternative to calculate k_{off} is to use the k_{on} value and the K_D obtained from equilibrium. Values obtained that way are very similar to those obtained from fitting to first-order decay with an offset (third and fourth columns in Table 2). This result supports the reliability of the values obtained from fitting.

Additionally, a simple but efficient self-consistency test of SPR data consists in comparing K_D constants obtained from different approaches: equilibrium and kinetic analysis [23]. From Tables 1 and 2 it is apparent that all K_D estimated by equilibrium analysis employing Langmuir or Scatchard plots were identical

Table 1
Equilibrium analysis for the three aptamers under study employing two approaches: Scatchard plot and Langmuir binding isotherm.

Equilibrium analysis					
Aptamer	**Equation**	K_D **(nM)**[a]	R_{max} **(m°)**[a]	K_D **(nM)**[b]	R_{max} **(m°)**[b]
ATA	$R_{eq}/[ATA]_{free}(m^\circ\ M^{-1}) = -(83\pm6)\times10^5\ (M^{-1})R_{eq}(m^\circ)+(44\pm2)\times10^7\ (m^\circ\ M^{-1})$; $r=0.994$	116 ± 8	51 ± 6	130 ± 20	52 ± 5
FATA	$R_{eq}/[FATA]_{free}(m^\circ\ M^{-1}) = -(44\pm5)\times10^5\ (M^{-1})\ R_{eq}(m^\circ)+(25\pm2)\times10^7\ (m^\circ\ M^{-1})$; $r=0.99$	210 ± 30	58 ± 6	170 ± 50	46 ± 9
NMATA	$R_{eq}/[NMATA]_{free}(m^\circ\ M^{-1}) = -(19\pm1)\times10^6\ (M^{-1})\ R_{eq}(m^\circ)+(104\pm4)\times10^7\ (m^\circ\ M^{-1})$; $r=0.995$	50 ± 20	60 ± 10	60 ± 40	60 ± 10

[a] Scatchard plot.
[b] Langmuir Binding Isotherm.

Table 2
Kinetic rate constants and dissociation constants calculated from kinetic analysis for the three aptamers under study.

Kinetic analysis				
Aptamer	k_{on} $(Ms)^{-1}$	k_{off} (s^{-1})[a]	k_{off} (s^{-1})[b]	K_D (nM)
ATA	$(12\pm2)\times10^4$	0.017 ± 0.001	0.014 ± 0.003	140 ± 30
FATA	$(93\pm3)\times10^3$	0.018 ± 0.002	0.020 ± 0.003	190 ± 30
NMATA	$(14\pm4)\times10^4$	0.013 ± 0.003	0.007 ± 0.004	90 ± 40

[a] k_{off} from dissociation fitting including offset.
[b] k_{off} from the expression $k_{off}=K_Dk_{on}$.

taking into account the experimental error and also equal to that obtained by the kinetics analysis. This simple test is a proof that helps to estimate the rightness of the data obtained.

In general, mean values from kinetic data make differences in affinity less distinct than from equilibrium values, but kinetic measurements have a larger associated error. Despite this, the same unambiguous trend is also observed within the experimental error. The lowest value corresponded to NMATA (below 100 nM) confirming the superior affinity of the native aptamer and the highest value corresponded to the FATA.

The affinity constant of the complex tobramycin and the unmodified anti-tobramycin aptamer, NMATA, was previously estimated [15]. Pyrene-labeled tobramycin was employed for performing quenching experiments under conditions where a 1:2 stoichiometry was found. Values of $K_{D1}=9$ nM and $K_{D2}=2.7$ μM were reported. K_{D1} is among the lowest values reported for an interaction between an aptamer and a small molecule rivaling with those of larger molecules such as proteins, which possesses a larger number of binding sites [24]. Typical K_D values for small molecules are in the subμM to μM range. The K_D value for NMATA reported in this work is more than one order of magnitude higher than the previously reported but still low for a small molecule. The difference can be attributed to the fact that the quenching experiments were carried out in solution. On the other hand, a much higher affinity constant value of $K_D=1.1$ μM was reported for NMATA–tobramycin complex carrying out SPR measurements [25]. In that study the aptamer was immobilized on the SPR sensor through biotin–streptavidin linkage. The use of a labeled aptamer on the surface as well as the use of an affinity buffer different from that it was used in the original aptamer selection can account for the significant differences in affinity. In addition to this, a very quick dissociation was observed indicating that the complex formed is not as stable as that generated with the configuration assayed in our work.

It was reported that ATA is also able to bind neomycin B, another aminoglycoside antibiotic and the anti-neomycin aptamer also recognize tobramycin [13]. This finding was attributed to the similar 3D structure of both aptamers and the way of encapsulating the antibiotic for binding. As a consequence the molecular recognition would be more related to the structure than to the sequence. If this holds true, similar K_D would be expected. However, both K_D values evaluated from SPR measurements differ in one order of magnitude. Neomycin B binds to its aptamer with a K_D of 1.24 ± 0.03 μM [12], suggesting that sequence also plays a role in the recognition event.

4. Conclusions

With the aim of taking advantage of the unique features of RNA aptamers as molecular recognition elements when dealing with real complex samples, modified aptamers can be used to avoid its degradation caused by nucleases. However, the extent of the affinity change after modification has to be quantified to ensure the proper performance of the tailored aptamer because the final activity is difficult to predict. In fact, both enhancement and loss in affinity has been reported. Herein the system tobramycin anti-tobramycin aptamer was taken as a model. The 27-mer RNA natural anti-tobramycin aptamer was chemically modified by introducing a 2′-*O*Me group instead of 2′-OH in the ribose moiety of the RNA structure.

SPR was employed for evaluating the affinity of three different RNA anti-tobramycin aptamers: the natural RNA sequence and two modified RNA aptamers, which differ in the modification of only a single base. A reverse configuration to what is often used was adopted to maximize SPR signal (immobilization of the small molecule maintaining the large one in solution) and hence, the accuracy of the kinetic and binding parameters evaluated.

In our case, the introduction of the selected internal modification altered the affinity of the aptamer towards its target molecule, tobramycin. A slight loss in the affinity is observed for both modified aptamers, which do not preclude the application of such modified aptamers as molecular recognition tools.

Acknowledgments

E.G.F. and N.S.A, thank to Spanish Government for a predoctoral grant and a Ramón y Cajal contract, respectively. This work has been financed by Project CTQ2008-02429 granted to "Grupos Consolidados" and the European Regional Development Fund.

Appendix A. Supporting information

Supplementary data associated with this article can be found in the online version at http://dx.doi.org/10.1016/j.talanta.2012.07.019.

References

[1] C. Tuerk, L. Gold, Science 249 (1990) 505–510.
[2] A.D. Ellington, J.W. Szostak, Nature 346 (1990) 818–822.
[3] E. Luzi, M. Minunni, S. Tombelli, M. Mascini, Trends. Anal. Chem. 22 (2003) 810–818.
[4] D.J. King, S.E. Bassett, X. Li, S.A. Fennewald, N.K. Herzog, B.A. Luxon, R. Shope, D.G. Gorenstein, Biochemistry 41 (2002) 9696–9706.
[5] C. Wilson, A.D. Keefe, Curr. Opin. Chem. Biol. 10 (2006) 607–614.
[6] W. Kusser, Rev. Mol. Biotechnol. 74 (2000) 27–38.
[7] S.D. Jayasena, Clin. Chem. 45 (1999) 1628–1650.
[8] P.E. Burmeister, S.D. Lewis, R.F. Silva, J.R. Preiss, L.R. Horwitz, P.S. Pendergrast, T.G. McCauley, J.C. Kurz, D.M. Epstein, C. Wilson, A.D. Keefe, Chem. Biol. 12 (2005) 25–33.
[9] F. Darfeuille, A. Arzumanov, M.J. Gait, C.D. Primo, J.J. Toulme, Biochemistry 41 (2002) 12186–12192.
[10] L.S. Green, D. Jellinek, C. Bell, L.A. Beebe, B.D. Feistner, S.C. Gill, F.M. Jucker, N. Janjic, Chem. Biol. 2 (1995) 683–695.
[11] N. de-los-Santos-Álvarez, M.J. Lobo-Castañón, A.J. Miranda-Ordieres, P. Tuñón-Blanco, J. Am. Chem. Soc. 129 (2007) 3808–3809.
[12] N. de-los-Santos-Álvarez, M.J. Lobo-Castañón, A.J. Miranda-Ordieres, P. Tuñón-Blanco, Biosens. Bioelectron. 24 (2009) 2547–2553.
[13] E. González-Fernández, N. de-los-Santos-Álvarez, M.J. Lobo-Castañón, A.J. Miranda-Ordieres, P. Tuñón-Blanco, Biosens. Bioelectron. 26 (2011) 2354–2360.
[14] L.C. Jiang, A.K. Suri, R. Fiala, D.J. Patel, Chem. Biol. 4 (1997) 35–50.
[15] Y. Wang, R.R. Rando, Chem. Biol. 2 (1995) 281–290.
[16] D.P. Morse, Biochem. Biophys. Res. Commun. 359 (2007) 94–101.
[17] P.W. Goertz, J.C. Cox, A.D. Ellington, J. Assoc. Lab. Autom. 9 (2004) 150–154.
[18] K.M. Song, M. Cho, H. Jo, K. Min, S.H. Jeon, T. Kim, M.S. Han, J.K. Ku, C. Ban, Anal. Biochem. 415 (2011) 175–181.
[19] D.J. O'Shannessy, D.J. Winzor, Anal. Biochem. 236 (1996) 275–283.
[20] T.M. Davis, W.D. Wilson, Methods Enzymol. 340 (2001) 22–51.
[21] N.J. de Mol, E. Plomp, M.J.E. Fischer, R. Ruijtenbeek, Anal. Biochem. 279 (2000) 61–70.
[22] P.R. Edwards, C.H. Maule, R.J. Leatherbarrow, D.J. Winzor, Anal. Biochem. 263 (1998) 1–12.
[23] P. Schuck, A.P. Minton, Trends Biochem. Sci. 21 (1996) 458–460.
[24] R. Stoltenburg, C. Reinemann, B. Strehlitz, Biomol. Eng. 24 (2007) 381–403.
[25] S.H.L. Verhelst, P.J.A. Michiels, G.A. van der Marel, C.A.A. van Boeckel, J.H. van Boom, ChemBioChem 5 (2004) 937–942.